

Contents lists available at ScienceDirect

Palaeogeography, Palaeoclimatology, Palaeoecology

journal homepage: www.elsevier.com/locate/palaeo





Evolutionary and biogeographic implications of an Erycine snake (Serpentes, Erycidae, *Eryx*) from the Upper Miocene of the Linxia Basin, Gansu Province, China

Jingsong Shi a,b,c,d,e,*, Qiang Li a,c,e, Thomas A. Stidham a,c,e, Chi Zhang a,c,e, Qigao Jiangzuo a,c,e,f, Mo Chen b,d, Xijun Ni a,c,e

- ^a Key Laboratory of Vertebrate Evolution and Human Origins of Chinese Academy of Sciences, Institute of Vertebrate Paleontology and Paleoanthropology, Beijing 100044, China
- ^b Institute of Zoology, Chinese Academy of Sciences, Beijing 100101, China
- ^c University of Chinese Academy of Sciences, 100044 Beijing, China
- d State Key Laboratory of Palaeobiology and Stratigraphy, Nanjing Institute of Geology and Palaeontology and Center for Excellence in Life and Paleoenvironment, Chinese Academy of Sciences, Nanjing 210008, China
- e Center for Excellence in Life and Paleoenvironment, Beijing 100044, China
- f Key Laboratory of Orogenic Belts and Crustal Evolution of Ministry of Education, School of Earth and Space Sciences, Peking University, Beijing 100871, China

ARTICLEINFO

Editor: Dr. Howard Falcon-Lang

Keywords: Aridification Late Miocene Qinghai-Tibet Plateau Sand boa Cenzoic snake fossil

ABSTRACT

The partial skeleton of a fossil snake is described from the Upper Miocene "Liushu" Formation of the Linxia Basin, Gansu Province, in the northeastern Tibetan Plateau of China. Material preserves rare cranial materials of the palatomaxillary arch, in addition to a series of vertebrae, represents a new species of erycine sand boa, *Eryx linxiaensis* sp. nov., the first fossil record of the superfamily Booidea in China. Combined phylogenetic analysis of osteological, ecological, and molecular data places this new extinct species within the crown clade *Eryx* as the sister species to the African *E. colubrinus*, with an average divergence time inferred as ~8.1 Ma. *Eryx linxiaensis* sp. nov. differs from the congeneric species by the combination of a series of morphological characters including the slightly dorsoventrally thickened anterior part of the maxilla, eleven maxillary teeth decrease in size posteriorly, more than five pterygoid teeth, relatively elongated middle trunk vertebrae with obvious haemal keel on the centrum, and short neural spine without a thickened dorsal edge. Multiple linear regressions of four vertebral measurements against the body size of extant specimens using an allometric model provide an estimated minimum total body length of c. 694 mm. Estimated species divergence times across the phylogenetic tree support intercontinental dispersals and overall radiation of the clade through the Miocene, potentially tied to increased aridification during parts of the Miocene. Our analysis also suggests that the *Eryx* crown clade evolved in Africa with at least three intercontinental dispersal events between African and Eurasian continents during the Miocene.

1. Introduction

Erycines (or sand boas of the genus *Eryx*, family Erycidae) are a group of pudgy terrestrial snakes having rather stubby tails and specialized shovel-shaped snouts suited to their burrowing lifestyle. Based on recent molecular phylogenetic studies, the extant family Erycidae contains only one monotypic genus, *Eryx* (Pyron et al., 2014a, 2014b; Zaher et al., 2019; Eskandarzadeh et al., 2013, 2020a, 2020b). Members of this clade mainly inhabit desert and steppe habitats where

they feed on a wide variety of small vertebrates, such as rodents, lizards, and birds (Kluge, 1993; Zhao et al., 1998; Zhao, 2006; Cundall and Irish, 2008).

Extant species of *Eryx* are widely distributed across the Old World, mainly in central and western Asia (e.g., *E. elegans*, *E. jayakari*, *E. johnii*, *E. miliaris*, and *E. conicus*) and Africa (e.g., *E. mulleri* and *E. colubrinus*). *Eryx jaculus* occupies the widest known geographic range, including Asia, Europe, and Africa (Rage, 1982; Kluge, 1993; Eskandarzadeh et al., 2013, 2020a, 2020b; Uetz and Hallermann, 2022).

E-mail address: shijingsong@ivpp.ac.cn (J. Shi).

^{*} Corresponding author at Key Laboratory of Vertebrate Evolution and Human Origins, Institute of Vertebrate Paleontology and Paleoanthropology, Chinese Academy of Sciences, Beijing 100044, China.

In recent decades, only one species, *E. miliaris* has been recorded in northwestern China (see below for the discussion on its synonym, *E. tataricus*), in the area north of the Yellow River, provinces of Inner Mongolia, Ningxia, Gansu, and Xinjiang (Fig. 1, Zhao et al., 1998; Yao,

2004; Zhao, 2006).

Published studies on the phylogenetic relationships of erycines have been based largely on morphological (Rage, 1977; Rieppel, 1978; Kluge, 1993) or molecular data (Pyron et al., 2013, 2014a, 2014b; Reynolds



Fig. 1. Map of Eastern Asia, showing the type locality of *Eryx linxiaensis* sp. nov. (Shangwangjia Village Maijiaxiang Town, Guanghe County, Linxia Hui Autonomous Prefecture, Gansu Province, China, red circle), with the collection localities of some extant *E. miliaris* (green triangles). The base map is provided by the Ministry of Natural Resources of the People's Republic of China (http://bzdt.ch.mnr.gov.cn/) with its censor code labeled at the bottom-left of the map. (For interpretation of the references to colour in this figure legend, the reader is referred to the web version of this article.)

et al., 2014, Eskandarzadeh et al., 2020a), and they revised the taxonomic relationships within the family Erycidae. Some of those changes include recognizing *E. tataricus* as a junior synonym of *E. miliaris*, and the description of a new species, *E. sistanensis* (Eskandarzadeh et al., 2020b). As Reynolds et al. (2014) discussed, the *Eryx* sand boas display interesting biogeographic patterns, and previous molecular phylogenetic studies hypothesized at least two dispersal events between Africa and Asia. However, the divergence dates within these clades have not yet been estimated because of some phylogenetic uncertainty, poor knowledge of their temporal distribution, and the near absence of total-evidence phylogenetic studies including fossil data.

The fossil records of extinct erycines (*Eryx sensu lato*) are quite rich throughout the Cenozoic Old World, including *Falseryx* and *Paleryx* from the Late Eocene of Egypt and England (Hecht and Hoffstetter, 1962; Nel et al., 1999; Mccartney and Seiffert, 2015), *Bransateryx* from the Middle/Late Pliocene (MN 15/16) of Spain and Oligocene of Germany (Szyndlar, 1994), *Albaneryx* from the Middle Miocene of France, unidentified erycine from Late Miocene Athens, Greece (Georgalis, 2019), and *Cadurceryx* from the Eocene of France and England (Hoffstetter and Rage, 1972; Szyndlar and Schleich, 1994). Note that recent studies suggested excluding *Flaseryx* and *Paleryx* from "erycine" snakes, see Georgalis (2019) and Georgalis et al. (2021).

The earliest fossil record of *Eryx sensu stricto* is based on the well-preserved trunk and caudal vertebrae from the Ayakoz locality in Kazakhstan with their age correlated as Neogene Mammal Zone MN 4 to MN 5 (late Early Miocene, Malakhov, 2005). Recently, that correlation was shifted to the earliest Miocene (Aquitanian; MN 1–2, Vasilyan et al., 2017).

Other fossils attributed to *Eryx* (including its synonym *Gongylophis*) are known from Old World Neogene and Quaternary sites, such as the Miocene and Quaternary of Europe (Szyndlar, 1991; Szyndlar and Schleich, 1994), the Early Miocene of Czech Republic (MN 4 Szyndlar, 1987) and Spain (Murelaga et al., 2002), and the late Early Miocene of Saudi Arabia (Rage, 1982) and Central Mongolia (Bo¨hme, 2007). Only in a few cases were species identified, including extinct *E. primitivus* from the Early Pliocene of Spain (Gorafe 5, MN 15, Szyndlar and Schleich, 1994) and *E. jaculus* from the Quaternary of Greece (Szyndlar, 1991). With these known records, the fossils point to a Miocene radiation of the clade. However, most of these erycine fossils preserve only the trunk or caudal vertebrae, and no cranial elements have been reported previously except for a left palatine of *Bransateryx vireti* (Szyndlar, 1994). It is difficult to include such materials in a total-evidence phylogenetic analysis.

Specimens of fossil snakes in China are extremely rare and most have been marked only with brief reports of colubrid snakes such as those found at the 'Peking Man' site of Middle Pleistocene Zhoukuodian, Beijing (Bien, 1934). The first-reported new taxon of Chinese fossil snake is *Mionatrix diatomus*, which includes two near-complete skeletons from the late Early Miocene diatomaceous beds in Shanwang County, Weifang City, Shandong Province (Sun, 1961). Other more recently reported fossil snakes include *Elaphe* sp. from the Early Pleistocene of Renzidong Cave, Fanchang County, Anhui Province (Mead et al., 2016), in addition to fossil colubrids and pit vipers from the Early Pliocene of Zhumadian, Henan (Shi and Li, 2023) and Middle-Late Pleistocene of Qinhuangdao, Hebei Province (Chen et al., 2019).

The Linxia Basin is an intramountain basin lying on the northeastern edge of the Qinghai-Tibet Plateau, the southern part of Gansu Province, with an average current elevation of ~2000–2400 m (Deng et al., 2013a, 2013b; Zhang et al., 2019). The extant fauna of the Linxia Basin is Palearctic, and the area is largely composed of plateau grasslands. The climate is semi-humid and cool, typical for the northeastern edge of the Qinghai-Tibet Plateau in modern times (Deng, 2006; Deng et al., 2013a, 2013b, 2023; Wang and Qiu, 2018; Zhang et al., 2019). The extant herpetofauna of the Linxia Basin and the adjacent region include species endemic to the Qinghai-Tibet Plateau and Hengduanshan Mountains (e. g., Gloydius liupanensis, Sphenomorphus indicus, and Scincella potanini),

along with a few widely-distributed Palearctic species, including *Elaphe dione* and *Rhabdophis tigrinus* (Wang et al., 1981). Extant xerophilous species, such as erycines or toad-headed lizards have never been reported in this area (Wang et al., 1981; Yao, 2004).

The Linxia Basin yields relatively abundant and diverse Cenozoic vertebrate fossils, particularly mammalian fossils. These vertebrate fossils include four faunas: a Late Oligocene Dzungariotherium fauna, a middle Miocene Platybelodon fauna, a Late Miocene Hipparion fauna, and an Early Pleistocene Equus fauna (Deng, 2006; Deng et al., 2013a, 2013b; Deng et al., 2019; Zhang et al., 2019). Of these, the Hipparion fauna includes diverse fossil mammals (e.g., Hipparion coelophyes, Plesiogulo brachygnathus, Pararhizomys hipparionum, Pseudorhizomys indigenus) and a growing list of fossil bird taxa (e.g., Gansugyps linxiaensis, Struthio linxiaensis, Miosurnia diurna, and Linxiavis inaguosus, Hou, 2005; Deng, 2006, 2007; Deng et al., 2013a, 2013b, 2019, 2021, 2023; Zhang et al., 2009; Wang and Qiu, 2018; Zhang et al., 2019; Li et al., 2020, 2022a, 2022b). This Late Miocene fauna points to the past presence of a relatively open and subarid grassland/steppe environment for the Linxia Basin, likely similar to the current savannahs of sub-Saharan Africa (Hou, 2005; Deng, 2006; Deng et al., 2013a, 2013b, 2019; Zhang et al., 2009). Recent studies of the fossil sandgrouse, diurnal owl, and ostrich specimens from the Linxia Basin further suggest an arid paleoenvironment (Li et al., 2020, 2021a, b, 2022a, b).

In contrast to the other vertebrate fossils, the fossil herpetofauna in the Linxia Basin are few except for some unidentified colubrids. The discovery of a fossil erycid snake provides further evidence of a dry paleoenvironment during the Late Miocene along the northeastern edge of the Qinghai-Tibet Plateau. As a step forward in our understanding of the evolution of the erycines and adding knowledge of the extinct snake fauna in China, we report the first fossil erycine from the Linxia Basin and implement a total-evidence phylogenetic analysis, in order to examine the systematic position of the new species and reconstruct likely biogeographic (intercontinental) dispersal patterns of the Old World erycid snakes.

2. Material and methods

2.1. Abbreviation

FMNH: Field Museum of Natural History (Zoology), Chicago, USA; IVPP: Institute of Vertebrate Paleontology and Paleoanthropology, Beijing, China; CAS: Chinese Academic of Sciences, China; YPM: Vertebrate Zoology Division: Herpetology, Yale Peabody Museum, New Haven, USA

2.2. Material

The holotype material (IVPP V 27593) is from the "Liushu" Formation of the Linxia Basin in Gansu Province, China (Fig. 1). Fossilized snake skeletal elements were entombed together with an almost complete skeleton of *Pseudorhizomys indigenus* (IVPP V 23698, ESM 1. Fig. S1), surrounded by reddish clay. The tooth sockets and the neural canals of the vertebrae are filled with a combination of reddish clay, gypsum, and calcites.

The new species is represented by an incomplete skeleton. Given the size and morphology of these fossil remains and their proximity to one another, they probably derive from one adult (or subadult) individual. The preserved parts include its near-complete left maxilla, the caudal segment of its right maxilla, the middle segment of its left pterygoid, in addition to 62 trunk vertebrae (most of them are damaged), two poorly preserved caudal vertebrae, and some rib fragments.

The accessions of the osteological specimens or figures of the extant erycid snakes that used for the comparison in this study are listed in ESM 1

2.3. Morphological measurements

The morphological characters and terminology used to describe the vertebrae follow Szyndlar (1994), LaDuke (1991), Holman (2000), and Cundall and Irish (2008). The regional subdivision of the entire snake vertebral column follows LaDuke (1991). The measurements in this study were taken with 0–200 mm vernier calipers to the nearest 0.1 mm following Szyndlar (1994).

2 3 1 Maxilla

MxD: maxilla depth, the depth of the dorsoventrally widest part of the maxilla in the lateral view; MxL: maxilla length, from the anterior tip of the maxilla to the posterior end of the ectopterygoid process of the maxilla; MxW: maxilla mediolateral width, the horizontal distance from the labial margin to the lingual-medial tip of the palatine process of the maxilla in the dorsal view. The maxillary teeth were counted based on the number of tooth bases adding empty tooth sockets.

2.3.2. Pterygoid

PtL: pterygoid anteroposterior length, from the anterior tip of the pterygoid to the caudal end of the pterygoid; PtW: pterygoid width, the mediolaterally widest distance from the medial transverse process of the pterygoid to the lateral margin of the ectopterygoid process of the pterygoid. The pterygoid teeth were counted based on the number of tooth bases adding tooth sockets.

2.3.3. Vertebra

CL: centrum anteroposterior length, from the anterior concavity of the cotyle to the posterior end of the condyle; CTH: cotyle height, the highest vertical diameter of the cotyle; CTW: cotyle width, the longest horizontal diameter of the cotyle; HL: head length, from the snout's tip to the mandible's posterior margin; HW: head width, the maximum width of the caudal end of the mandibles; NAW: neural arch width, the minimum horizontal distance between the interzygapophyseal ridges; PR-PO: prezygapophysis-postzygapophysis distance, the maximum distance between the prezygapophysis and postzygapophysis; PRD: prezygapophyseal distance, the transverse distance between two prezygapophyseal processes; POD: postzygapophyseal distance, the transverse distance between two postzygapophyseal processes; and VH: vertebra height (depth), the largest dorsoventral distance of the vertebra. The morphological comparison between the fossil taxon and its extant congeneric species is shown in Table 1.

2.4. Body size estimation

Given that the size of a snake's vertebra is positively correlated to its body size, the latter can thus be predicted from vertebral dimensions since it evolved with the increasing size of vertebrae (Head et al., 2009., Shi et al., 2023). Thus, we used multiple linear regressions with an allometric model (logarithmic values of size), implemented by the 'lm()' function provided in R studio (Team, 2012). The error for size estimates was determined by subtracting the averaged regression coefficients from a perfect fit for extant taxa. In this study, four measurements of the most completely preserved structures of trunk vertebra, CL, NAW, POD, and PR-PO of the erycines were considered the dependent variables while SVL and TOL are considered independent variables. See Tables 2–3 for the measurements of the fossil materials and extant osteological specimens.

2.5. CT-scanning and three-dimensional reconstructions

The CT scanning was carried out with Nano-computerized tomography. Specimens were scanned using a GE v|tome|x m dual tube 300/180 kV system in IVPP, CAS. The specimens were scanned with an energy beam of 80 kV and a flux of $80 \times \mu A$ using a 360° rotation and then reconstructed into the 4096×4096 matrices of 1536 slices. The final CT

reconstructed skull images were exported with a minimum resolution of 6.10 μ m. The skull images were exported from the virtual 3D model which was reconstructed by Volume Graphics Studio 3.4 (Volume Graphics GmbH, 2017). The dataset of the 3D models included in this study is available online in the repository (ADMorph, Hou et al., 2020).

2.6. Systematic and phylogenetic analyses

2.6.1. Morphological, molecular, and ecological data

We downloaded available genetic sequence data in GenBank (Benson et al., 1990) across the currently recognized species in our study and identified nine loci that were broadly sampled in previous studies following Reynolds et al. (2014), Pyron et al. (2013a, 2014b), and Tonini et al. (2016), including two mitochondrial genes: cytochrome b (cytb, 996 bp after alignment) and the small subunits of the 16S mitochondrial ribosome gene (16S, 475 bp), adding six nuclear genes: recombination-activating protein 1 (RAG-1, 850 bp), oocyte maturation factor (c-mos, 465 bp), neutrophin-3 (NTF3, 495 bp), brain-derived neutrophic factor (BDNF, 670 bp), ornithine decarboxylase intron (ODC, 597 bp), and solute-carrier family 30 member 1 (SLC30A1, 513 bp).

Additionally, to assess the phylogenetic position of the new extinct species, 98 discrete morphological/ecological characters were included in the analysis: characters 1–75 are taken from Kluge (1993), while 76–98 are based on observations by Rieppel (1978), Tokar (1989), Scanferla et al. (2016), Smith and Scanferla (2021), and this study. The character list, including the explanation of these characters and their states, is presented in ESM 3. The discrete classified characters were treated as non-additive (Goloboff et al., 2006).

A final dataset comprised of 5159 characters scored across 19 operational taxa (17 extant species and one extinct species) was analyzed in this study, including 5061 bp of nucleotide sequence data, in addition to 98 morphological/ecological characters.

2.6.2. Phylogenetic analyses

Concerning the different evolutionary characters of each molecular marker, the dataset was split initially into 20 partitions by both gene and codon positions and then combined into 11 partitions taking advantage of the greedy algorithm provided by PartitionFinder 2.1.1 (Lanfear et al., 2012, 2016) to find similarly evolving partitions. The evolutional model of morphological data is set as Mkv + GAMMA. The evolutionary models assigned to each of the partitions by PartitionFinder are shown in Table 4.

The fossil records of the new taxon and *Eryx jaculus* (7.25–5.33 Ma: Szyndlar, 1994) were set for tip-date calibration while the divergence between *Charina* and *Lichanura* (~20–18.7 Ma, Head, 2015) was set as node-date calibration for uniform molecular clock according to Tedford et al. (2004) and Zhang et al. (2019). To root the tree properly, we enforced the constraint groups of the monophyletic group of the American clades of the family Boidae. The root age was assigned an offset-exponential prior with a mean of 35 Ma and a minimum of 30 Ma (Pyron et al., 2014a, 2014b).

A Bayesian phylogenetic analysis was performed using MrBayes 3.2.7 (Ronquist et al., 2012). The Markov chain Monte Carlo consisted of two independent runs with three heated chains and a single cold chain per run. Each run of 50 million was sampled every 1000 generations, and parameter estimates were plotted against generation. The first 25% of the samples were discarded as burn-in. Parameter estimates were plotted against generation (trace plot) and the effective sample size of each parameter was checked to be greater than 200. Topological convergence was checked based on the average standard deviation of split frequencies smaller than 0.005 (Zhang, 2019, 2021).

2.7. Ancestral geographic/state reconstruction

To better understand the origin, dispersal, and evolution of the

reproduction mode of the erycines, we recovered the biogeography and ecology of the family by mapping the stochastic characters across the time-calibrated phylogenetic tree. The distribution areas are set as stochastic characters which are shown in Table S1. We tested different models using the methods proposed in BioGeoBEARS (Matzke, 2013) implemented in the software RASP 4.2 (Yu et al., 2015; Yu et al., 2020). The detailed setting of biogeographic information is provided in ESM 2. Table S1). The best-fit model was chosen by corrected Akaike information criterion (AICc). For the reproduction modes, model selection was performed before stochastic character mapping. Three different models (equal-rates (ER), symmetric (SYM), and all-rates-different (ARD)) were fitted to the phylogenetic tree with "fitDiscrete" command in the R package Geiger (Pennell et al., 2014), and models were selected by corrected Akaike information criterion (AICc; Burnham et al., 2002). ASR analyses using stochastic character mapping were conducted with the "make.simmap" command in the R package phytools (Revell, 2012; Team, R.C, 2012) with 1000 simulations (Li et al., 2021a, 2021b; Li et al., 2022a, 2022b).

3. Systematic paleontology

Class Reptilia Laurenti, 1768 Order Squamata Oppel, 1811 Suborder Serpentes Linnaeus, 1758 Superfamily Booidea Gray, 1825 Family Erycidae Bonaparte, 1831 Genus *Eryx* Daudin, 1803

Eryx linxiaensis sp. nov. Shi, Li, Stidham, Zhang, Jiangzuo, Chen, and Ni, 2023.

ZooBank accession: 85621627-C53D-47B1-97C8-3D44CFADE7C4.

Etymology. The specific epithet refers to the Linxia Basin, where the holotype specimen was collected.

 ${\bf Holotype.~IVPP~V~27593},$ a series of partially preserved cranial and post-cranial elements:

IVPP V 27593–1, a near-complete left maxilla fragment (Fig. 2-A); IVPP V 27593–2, the caudal segment of the right maxilla (Fig. S2 in ESM 2); IVPP V 27593–3 a left pterygoid fragment (Fig. 3-A); IVPP V 27593–4 two articulated middle trunk vertebrae (Fig. 4-A); IVPP V 27593–5 two articulated post-cervical trunk vertebrae; IVPP V 27593–6 another middle trunk vertebra; IVPP V 27593–7 two articulated posterior (precaudal) trunk vertebrae; and IVPP V 27593–8 two articulated caudal vertebrae

3.1. Locality, horizon, and age

The collection site of the fossil erycine is near Shangwangjia Village

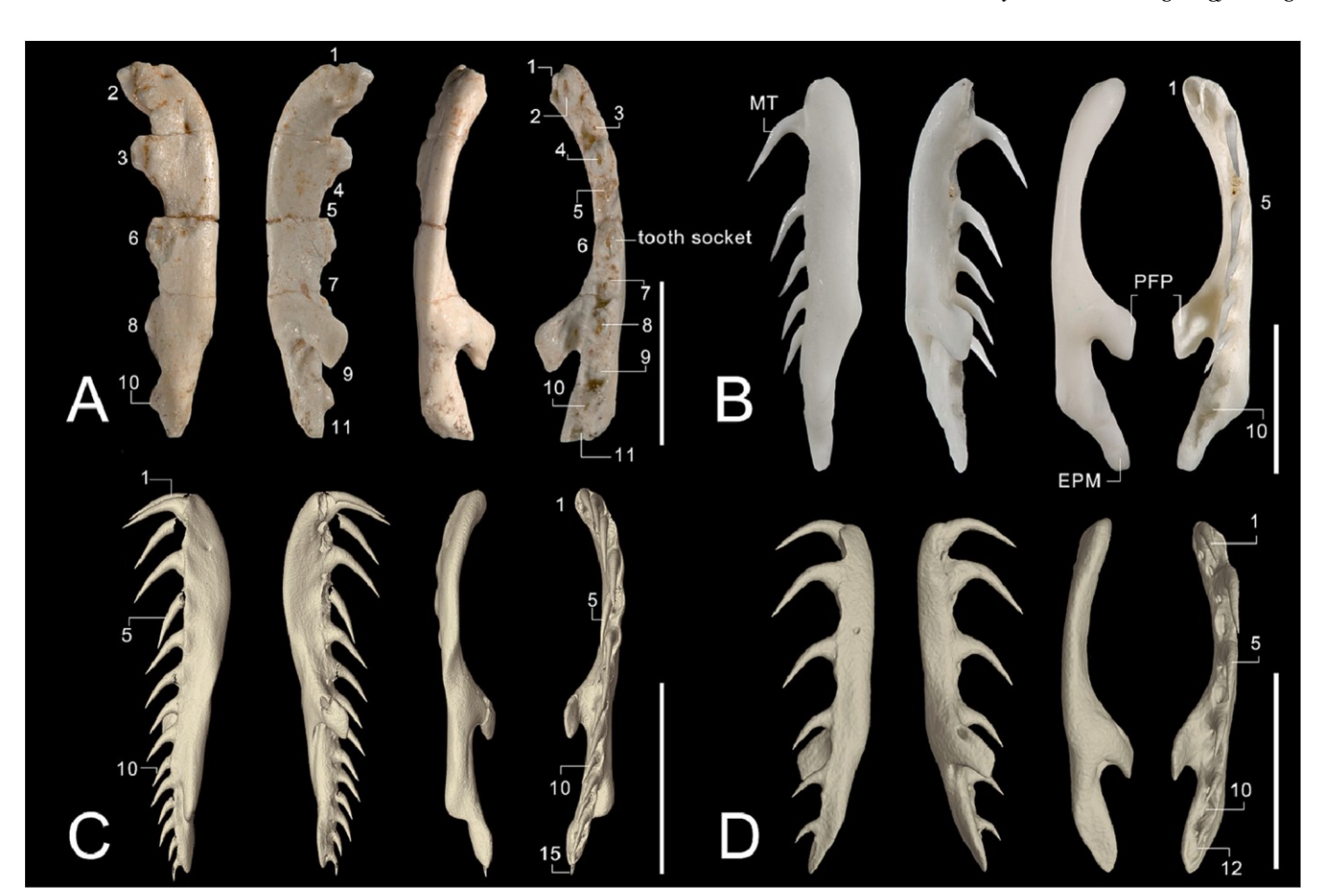
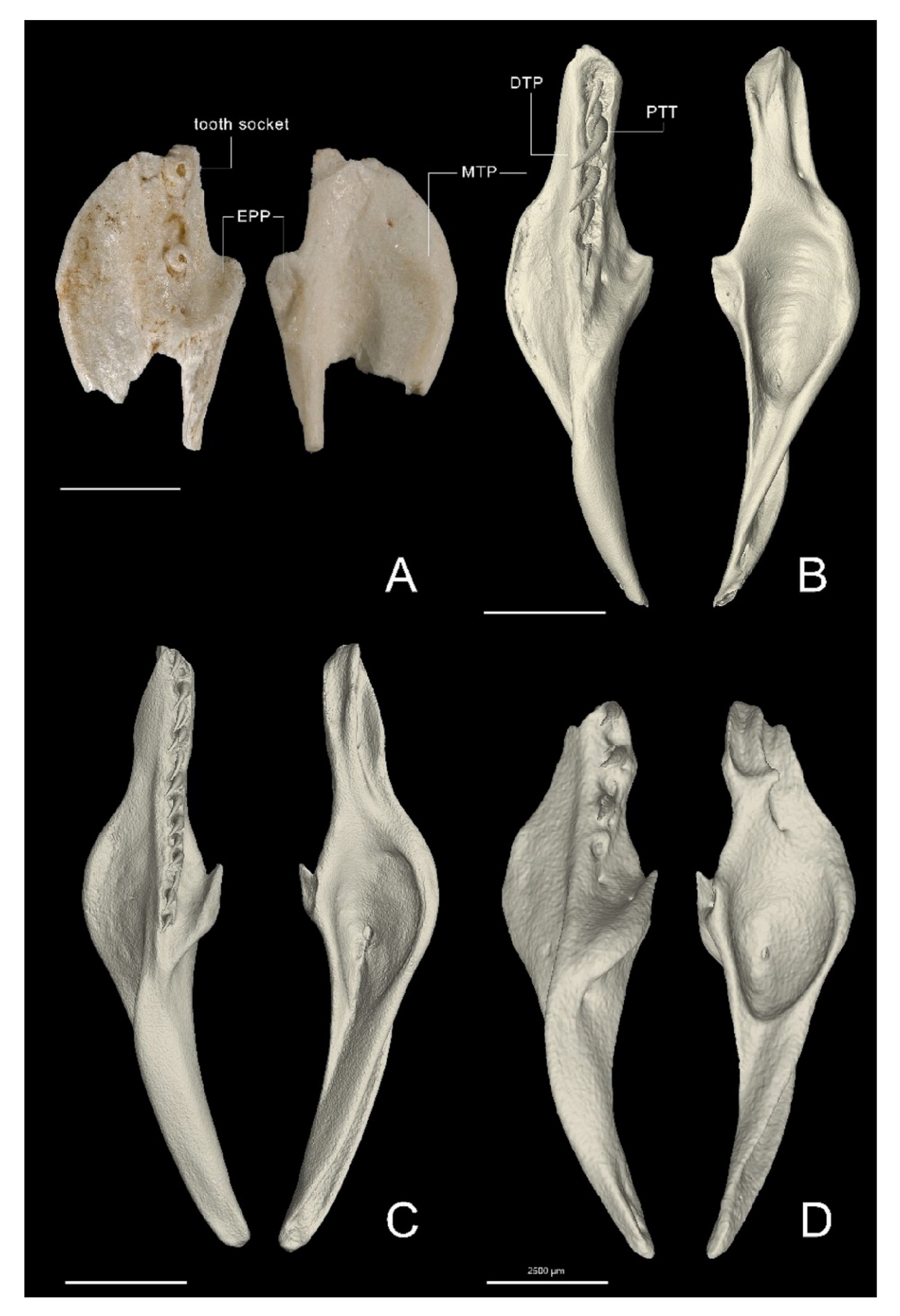


Fig. 2. Maxillae of Eryx linxiaensis sp. nov. and three extant species of Eryx (from left to right: labial, lingual, dorsal, and ventral views).

- A. complete left maxilla of *E. linxiaensis* sp. **nov.** (holotype, IVPP V 27593–1);
- B. left maxilla of extant E. miliaris from Xinjiang (IVPP OV 2728);
- C. right maxilla (horizontally mirrored) of extant E. conicus from India (IVPP OV 2741);
- D. horizontally mirrored right maxilla of extant *E. colubrinus* from Faiyum, Egypt (FMNH 63117, image from MorphoSource, Media ID: 000098517). Abbreviations

EPM, ectopterygoid process, MT maxillary tooth, and PFP prefrontal process. The numbers shown beside the teeth and tooth sockets indicate the tooth count of the maxillae. Scale bars = 5 mm



(caption on next page)

Fig. 3. Pterygoids of *Eryx linxiaensis* sp. **nov.** and the three-dimensional reconstructed model of three extant species of *Eryx* (left: ventral view; right: dorsal view). A. middle part of the left pterygoid of *E. linxiaensis* sp. **nov.** (holotype, IVPP V 27593–3);

- B. left pterygoid of extant E. miliaris from Xinjiang (IVPP OV 2728);
- C. left pterygoid of extant E. conicus from India (IVPP OV 2741);
- D. left pterygoid of extant *E. colubrinus* from Fayum, Egypt (FMNH 63117, image obtained from MorphoSource, Median ID: 000098517). Scale bars = 2.5 mm. Abbreviations: DTP dentigerous process of the pterygoid, EPP ectopterygoid process, MTP medial transverse processes of the pterygoid, and PTT pterygoid teeth

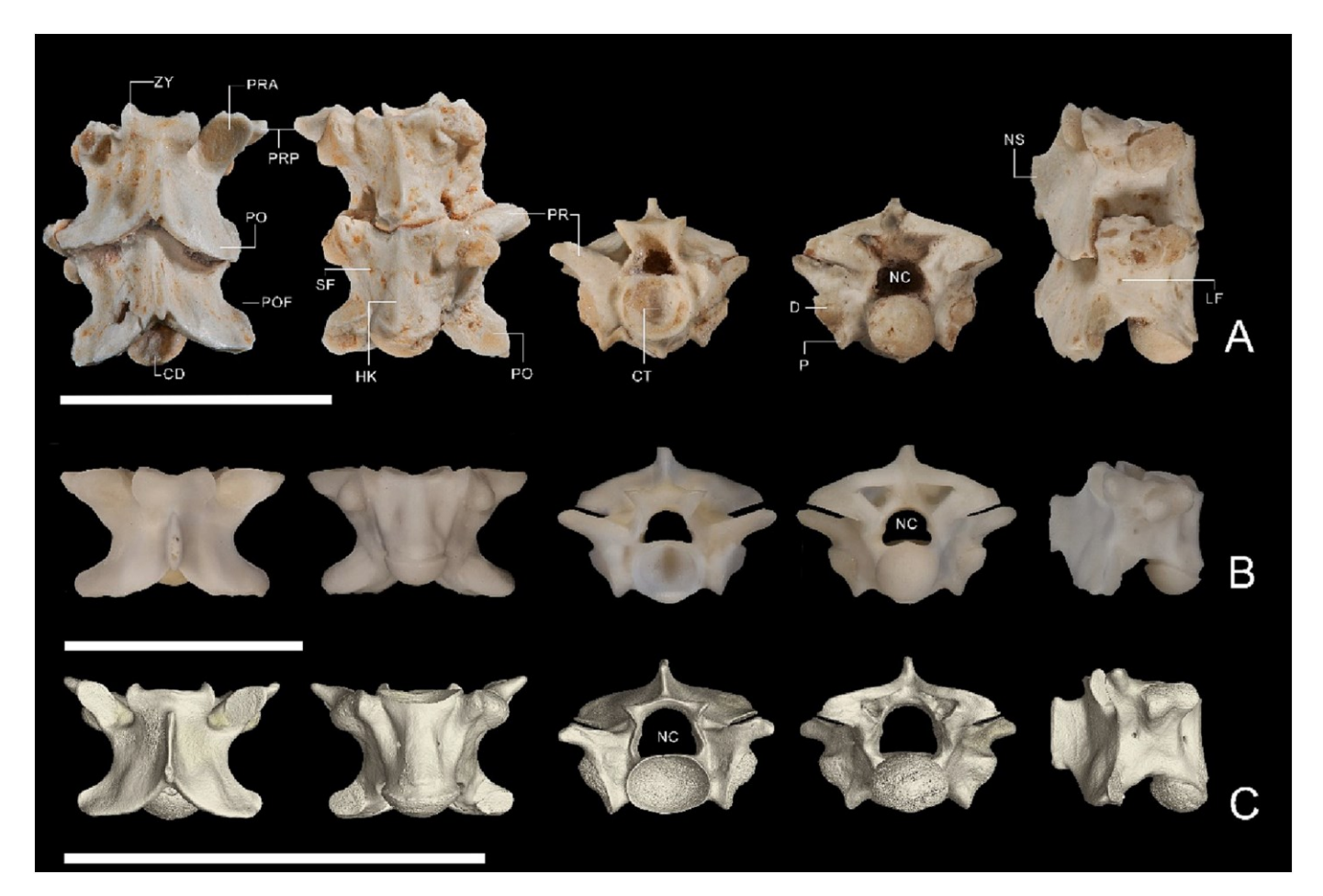


Fig. 4. Two articulated trunk vertebrae of *Eryx linxiaensis* sp. nov., compared to two extant *Eryx* species (from left to right: dorsal, ventral, anterior, posterior, and lateral views: dorsal view).

- A. Eryx linxiaensis sp. nov. (holotype, IVPP V 27593-4);
- B. Middle trunk vertebra (90th) of $E.\ miliaris$ from Xinjiang Province (IVPP OV 2728);
- C. Middle trunk vertebra E. conicus from India (IVPP OV 2741). Scale bars equal 10 mm.

Abbreviations: C centrum, CD condyle, CT cotyle, D diapophysis, HK haemal keel, LF, lateral foramina, NC neural canal, NS neural spine, P parapophysis, PO postzygapophysis, POF postzygapophysis facet, PRA prezygapophyseal articular facet, PRP prezygapophyseal accessory process, SF subcentral foramen, and ZY zygosphene

Maijiaxiang Town, Guanghe County, Linxia Hui Autonomous Prefecture, Gansu Province, China (Fig. 1). The fossil erycid snake is attributed to Yangjiashan Fauna (the upper strata of the "Liushu" Formation). The age of the new fossil is estimated as Late Miocene (~8–7.25 Ma) based on associated mammalian fauna (Deng, 2007; Deng et al., 2013a, 2013b, 2019, 2023; Wang and Qiu, 2018).

3.2. Diagnosis

Generally, the members of the genus *Eryx* can be recognized based on the presence of short and broad vertebral centra, and stubby neural spines, in addition to several other osteological synapomorphies, including 1) complete loss of all processes on the rostral end of the ectopterygoid; 2) presence of a medial ridge on the rostral end of the pterygoid that extends the palatopterygoid joint; 3) the maxillary

process of the palatine being caudally positioned; 4) the functional axis of the palato-pterygoid joint aligned in a line; 5) right posterior vidian canal larger than the left; 6) fewer than six palatine teeth; 7) the nasal process of premaxilla reduced or absent; 8) extension of the medial margin of the pterygoid; 9) the number of maxillary teeth ranges from nine to 14; and 10) relative anteroposteriorly shortened and anteriorly positioned neural spines (Kluge, 1993; Szyndlar and Schleich, 1994; Bo"hme, 2007; Cundall and Irish, 2008; Pyron et al., 2014a, 2014b).

Thus, we could attribute the partial fossil skeleton, IVPP V 27593 to the genus Eryx based on the shared presence of characters 2, 8, 9, and 10 in the holotype specimen.

Eryx linxiaensis sp. **nov.** can be distinguished from the genus *Calabaria* (African family Calabariidae) by the presence of palatine and pterygoid teeth (versus the absence of palatine and pterygoid teeth in *Calabaria*); from the extinct genus *Calamagras* by the anteriorly-

positioned thin neural spine (versus the thick cylindrical posteriorly-positioned neural spine in *Calamagras*, Rage, 1977; Bo hme, 2007); from *Corallus*, *Candoia*, and *Ungaliophis* by the presence of small maxillary teeth (versus the exceptionally long anterior maxillary teeth, Cundall and Irish, 2008); from *Lichanura* and *Exiliboa* by having fewer (eleven) maxillary teeth and rudimentary ectopterygoid process of the pterygoid (versus the presence of more than 15 maxillary teeth and a prominent ectopterygoid process in *Lichanura* and *Exiliboa*), and curved posterior end of the maxilla (versus straight posterior end in *Lichanura*); and from *Charina* by the convex medial margin of the pterygoid (versus the angulated in *Charina*).

3.3. Infrageneric comparison

Eryx linxiaensis sp. **nov.** can be differentiated from congeneric species using the combination of the following characters: 1) slightly dorsoventrally thickened anterior part and the vaulted anterodorsal edge of the maxilla; 2) eleven maxillary teeth, decreasing in height posteriorly; 3) more than five pterygoid teeth; 4) relatively elongated middle trunk vertebrae (CL/NAW = 0.88–0.91, PDD/PR-PO = 1.20–1.25) and posterior trunk vertebra (CL/NAW = 1.23, PDD/PR-PO = 0.80); 5) relatively short neural spines without a thickened dorsal

= 0.89); 5) relatively short neural spines without a thickened dorsal edge (NSL = 1.6–2.2); and 6) obvious haemal keels on the centrum.

Morphologically, *Eryx linxiaensis* sp. **nov.** shares many osteological similarities with *E. colubrinus*, a living species endemic to Africa, such as the moderate number of maxillary teeth, the undeveloped ectopterygoid process of the maxilla, the presence of a haemal keel on the vertebra, and the medially expanded medial transverse process of the pterygoid. On the other hand, *E. linxiaensis* sp. nov. differs from *E. miliaris*, a living species of Gansu, China, in many ways (see Table 1 and following comparisons).

For detailed comparison within the genus *Eryx*, *E. linxiaensis* sp. **nov.** differs from most extant species by the presence of trunk vertebrae with roughly equal length and width (versus the pudgy trunk vertebra with widths greater than their lengths as in other *Eryx* species) and anterior-thickened maxilla (versus the anteroposterior equal-heightened maxilla in most extant *Eryx* species except *E. conicus*).

Eryx linxiaensis sp. nov. differs from E. miliaris by having a curved maxilla and shorter blunter ectopterygoid process of the maxilla (versus relatively straight maxilla and elongated slender ectopterygoid process of the maxilla in E. miliaris); from E. colubrinus by the blunt and broad anterior edge of the maxilla, the presence of the haemal keels on the ventral side of middle trunk vertebrae (versus slender and slightly cupped anterior maxilla edge, lack of a haemal keel); from E. elegans, E. miliaris, and E. jaculus by having at least five pterygoid teeth (versus three pterygoid teeth in *E. elegans* and *E. jaculus*, four pterygoid teeth in E. miliaris); from E. conicus, E. jayakari, E. muelleri, and E. somalicus by having 11 maxillary teeth (versus seven maxillary teeth in E. somalicus, 11-13 in E. muelleri, 13 in E. jayakari and 13-18 in E. conicus); from E. jaculus E. muelleri and E. somalicus by the well-developed medial transverse process of the pterygoid (versus much reduced medial transverse processes in E. jaculus E. muelleri, and E. somalicus); and from E. johnii, E. jaculus, and E. miliaris by the presence of haemal keels on the trunk vertebrae (versus absence of the haemal keels in these species).

3.4. Description

3.4.1. Cranial elements

3.4.1.1. Maxillae. IVPP V 27593–1, the left maxillary bone includes three fragments and is almost complete. The right maxilla preserves only the caudal part. The left maxilla measures 21.4 mm in length, 4.7 mm at the mediolaterally widest part (positioned between the medial tip of the ectopterygoid process and the labial margin in dorsal view), and 4.1 mm at the dorsoventrally highest part (between the base of the fourth

maxillary tooth and the dorsal maxillary margin in the lateral view). The caudal part of the right maxillary fragment bears five tooth sockets. The palatine process and the ectopterygoid process are both preserved. In lateral view, compared to some extant Eryx species (e.g., E. miliaris and E. colubrinus), the anterior portion of the maxilla of the fossil Eryx becomes taller, ventral to the lateral apex of the prefrontal. The posterior tip is flattened. The anterodorsal ridge of the maxilla is slightly vaulted. In dorsal view, the anterior part of the maxilla is inclined medially. The prefrontal process of the maxilla is shaped as a nearly round-cornered rhombus and is moderately elongated and caudolaterally directed. The ectopterygoid process of the maxilla is almost merged with the caudal part of the maxilla and is slightly inclined medially. In ventral view, the five tooth bases and six tooth sockets suggest that the maxilla bears a total of 11 teeth, the second is the largest, and the teeth are reduced in height posteriorly from the second one. IVPP V 27593-2, the caudal segment of the right maxilla with its prefrontal and ectopterygoid processes completely preserved. In lateral and ventral views, the preserved segment bears seven teeth, including five tooth bases and two tooth sockets (Fig. S1).

3.4.1.2. Pterygoid. IVPP V 27593–3, the anteroposterior length of the preserved segment of the left pterygoid measures 13.7 mm. The anterior part of the dentigerous process and the caudal end of the pterygoid are crushed. The widest part of the pterygoid (the distance between the ectopterygoid process distal termination and the medial margin) measures 8.4 mm. The ectopterygoid process of the pterygoid is stubby and has an outline like a rounded right triangle in ventral view. The pterygoid-ectopterygoid articular facet is oval-shaped and extends to the palatine facet. The medial transverse process of the pterygoid is well developed. The process is in a semicircular shape. The anterodorsal part of the medial transverse process is flat, and without a noticeable curvature. The medial ridge of the pterygoid is slightly thickened. The dentigerous process of the pterygoid extends for about one tooth distance posterior to the caudal end of the ectopterygoid angular facet. The number of pterygoid teeth is unknown because of the crushed dentigerous process. However, the preserved tooth and tooth sockets indicate that there are likely more than five functional pterygoid teeth.

3.4.2. Postcranial skeleton elements

3.4.2.1. Middle trunk vertebrae. IVPP V 27593-4. The length and width of the vertebral centrum of the new species are roughly equal (CL/NAW = 0.91). The centrum length of these two articulated trunk vertebrae is 3.9 mm. The mediolateral distance between the bilateral prezygapophyses is 6.2 mm and the distance between the postzygapophyses is 6.0 mm. The distance between the prezygapophyses and postzygapophyses is 4.8 mm. In lateral view, the neural spine is moderately developed, with its anterior margin tilting slightly. Craniocaudally, the anterior margin of the neural spine originates at the anterior part of the neural arch. The craniocaudal length of the neural spine is about twothirds of the craniocaudal length of the neural arch. The caudal margin of the neural spine overhangs notably posteriorly, while the cranial margin is slightly anterior-inclined. In dorsal view, the outline of the trunk vertebra is squared-off, but with a constriction between the pre-and postzygapophyses (CL/NAW = 0.91). The anterior edge of the neural spine is near perpendicular to the centrum, while the posterior edge is shorter and slopes posteriorly. The dorsal border of the neural spine is slender, not thickened. The anterior and posterior parts are roughly equal in width. The zygosphene is blunt and robust, and the anterior margin of the zygosphene is divided into two lobes, both moderately developed. The lateral foramina are small and present on all of the trunk vertebrae. The parapophyseal and diapophyseal processes are large and strong. Both are similar in size. The paradiapophyses are kidney-shaped. The anterior border of the zygosphene is bilobate and slightly notched. The prezygapophyseal articular facet is oval. The

prezygapophyseal accessory process is quite stubby and blunt. The margin of the anteromedial notch of the neural arch is smooth. The epizygapophyseal spines are absent. The postzygapophyseal articular facets are oval in shape. The caudal margin of the condyle is not distinct from the centrum.

In ventral view, the haemal keels are moderately developed and present on most of the centra. The subcentral grooves lateral to the hypophyseal are shallow. The subcentral foramina are present lateral to the haemal keel. The anteroventral margin of the cotyle is slightly concave, forming a fovea. The zygosphene is rather lightly built. Its dorsal edge is slightly concave. The cotyle is suborbicular in outline. Its width is similar to that of the zygosphene. The paracotylar foramina are absent. The root of the prezygapophysis is thick. The tip of the prezygapophyses tilts anteriorly. The cross-section of the neural canal is subtriangular in outline. In posterior view, the neural arch is moderately vaulted. The zygantrum is triangular. The condyle is large and orbicular shaped (CTW/CTH = 1.17).

3.4.3. Intracolumnar variability

The posterior trunk vertebrae (IVPP V 27593–7) are notably anteroposteriorly elongated relative to the anterior or mid-body trunk vertebrae. The ratios between the centrum length and neural arch width (CL/NAW) in the former are much greater than those in the latter (1.23 versus 0.88–0.91), while the ratios between the postzygapophyseal distance and prezygapophyseal-postzygapophyseal distance (POD/PR-PO) in the former are much lower than those in the latter (0.89 versus 1.20–1.25). The haemal keels and subcentral ridges are more conspicuous in the posteriorly situated vertebrae than those in the anterior or mid-body trunk vertebrae.

3.5. Body size estimation

Multiple linear regressions using an allometric model (with logarithmic values of size) produced significant relationships between the body length (SVL and TOL) and four vertebra measurements (CL, NAW, POD, and PR-PO) within the extant specimens of the genus *Eryx*. Based on a preserved largest middle trunk vertebra of *E. linxiaensis* (IVPP V 27593–4), a minimum snout-vent length of 571.34 mm and a minimum total length of 694.32 mm were yielded by multiple linear regression

analysis of the vertebral measurements against body size. See Table 5 for the details of the multiple linear regression analysis.

3.6. Total-evidence phylogeny and biogeography

The topology of the Total-evidence phylogenetic tree resulting from our analysis is generally consistent with recent studies (Reynolds et al., 2014; Eskandarzadeh et al., 2020a, 2020b). *Calabria reinhardtii* is found as an early diverging taxon, and the individual species of *Eryx* form an exclusive monophyletic clade. The *Eryx* clade separated from the American lineages during the Oligocene and Early Miocene (estimated divergence date of 33.5–21.41 Ma, mean 26.89 Ma, Fig. 5).

However, the three species that occur in Africa do not form an exclusive clade. This result suggests multiple intercontinental dispersal events of Old World erycines into and/or out of Africa. The clade consisting of two oviparous species, *E. muelleri* from western Africa and *E. jayakari* from western Asia, is recovered as an early-diverging clade within *Eryx*. The extinct Chinese species, *E. linxiaensis* sp. nov. is recovered as the sister taxon to *E. colubrinus* from eastern Africa. The divergence time between these two species was inferred as (11.34–7.25 Ma, mean 8.12 Ma, Fig. 5). Additionally, five species from central and western Asia form a strongly supported monophyletic clade with an average divergence time of 10.12 Ma (12.89–7.85 Ma, Fig. 5), indicating clade diversification during the late Miocene.

As discussed by Kluge (1993) and Reynolds et al. (2014), Afro-Eurasian erycines exhibit interesting biogeographic patterns. The results of our historical biogeographic analysis point to at least three intercontinental dispersal events of the *Eryx* taxa between Africa and Asia. In addition, our results support an Old World origin of the *Eryx* crown clade. The divergence time between two oviparous species was estimated as 16.62–9.45 Ma (mean 12.7 Ma, Fig. 5), indicating the first dispersal event from western Africa to central western Asia likely occurred near the beginning of the late middle Miocene (Serravallian Stage). The occurrence of *E. linxiaensis* sp. nov. and its possible divergence from *E. colubrinus* is attributed to a second dispersal event from Africa during the Tortonian Stage, early Late Miocene (11.34–7.25 Ma, mean 8.12 Ma, Figs. 5 – 6). Another dispersal event is inferred as the infraspecific biogeographic spread of *E. jaculus*. However, we could not estimate this timing due to a lack of samples of *E. jaculus* from different

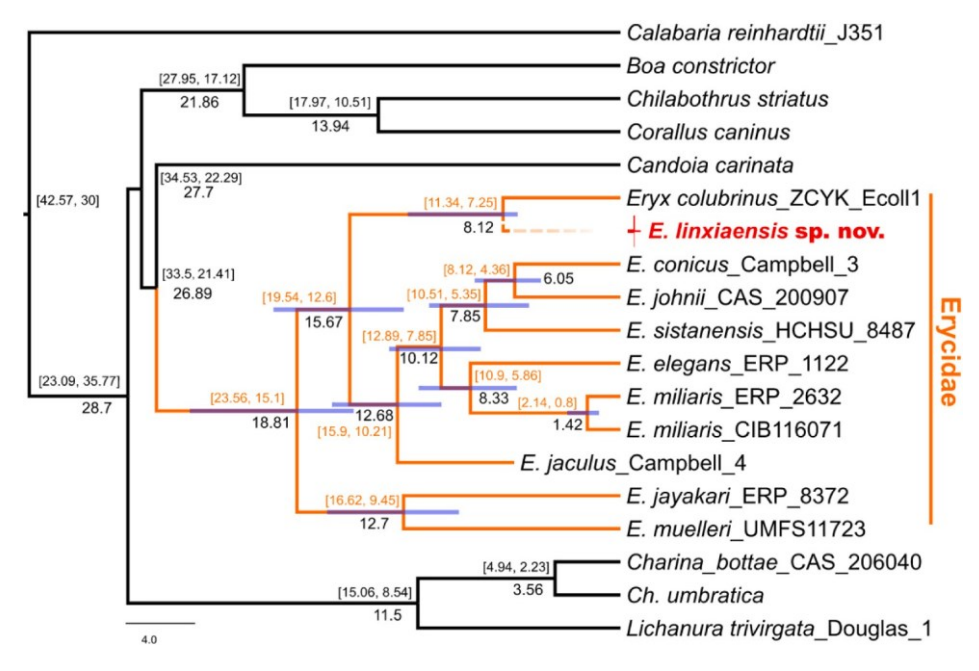


Fig. 5. Time-calibrated Bayesian total-evidence phylogenetic tree of the Old World sand boas *Eryx*. The divergence age estimates (95% highest posterior density intervals) are shown as node bars with the mean divergence age estimates shown below the nodes.

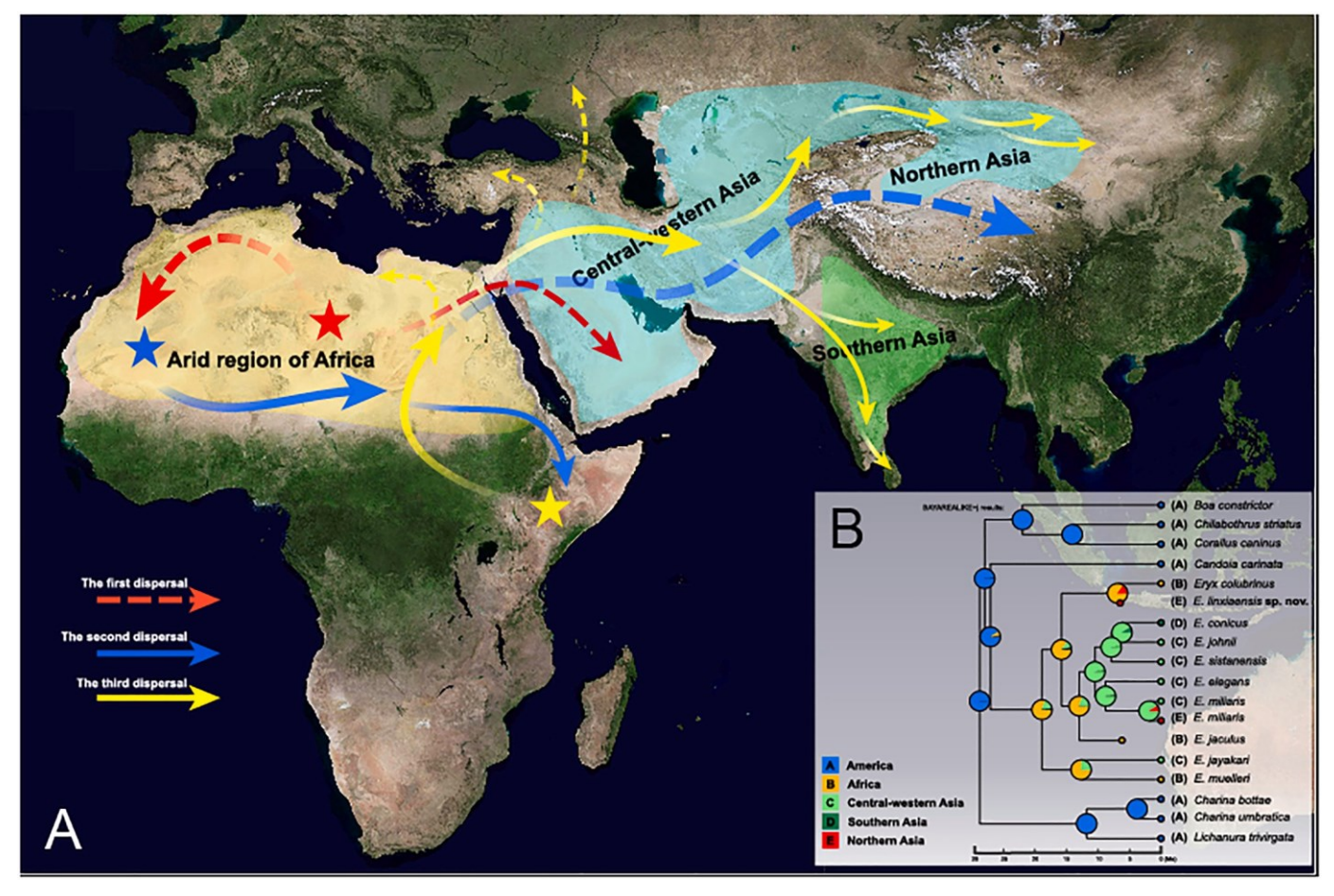


Fig. 6. Possible intercontinental dispersal routes of the Old World erycines during the Miocene (A), informed by ancestral geographic reconstruction (B).

continents.

While *Eryx linxiaensis* and *E. miliaris* are geographically close to one another, our phylogenetic results indicate a distant affiliation. The divergence time between the populations of *E. miliaris* from western Asia (Iran) and eastern Asia (Xinjiang Province) was estimated as late Early Pleistocene (2.14–0.8 Ma, mean 1.42 Ma), much younger than the occurrence of the fossil taxon, *E. linxiaensis* sp. nov. (Figs. 5–6).

4. Discussion

4.1. Ecology

Despite the earliest diverging position of the two oviparous species in the sand boa clade suggesting that their oviparity is relatively primitive, the result of the ancestral state reconstruction shows that the family Erycidae is likely to have originated with ovoviviparity and *Eryx lin-xiaensis* sp. **nov.** may have been ovoviviparous (ESM 2. Fig. S4). The diet of *E. linxiaensis* sp. **nov.** remains unknown even though the fossil is entombed together with a skeleton of *Pseudorhizomys indigenus*. The rodent may have been too big for the snake to consume as inferred from the great disparity between the snake and the rodent in body size (ESM 2. Fig. S2). Typical prey would have been smaller rodents and birds (Fig. 7).

4.2. Intercontinental dispersal of erycines

The hard collision between Arabia and Eurasia resulting in the gradual closure of the Tethyan Seaway between 13 and 17 Ma (Gülyüz et al., 2020; Sun et al., 2021; Wang et al., 2022), may have formed a land bridge between the Afro-Arabian and Eurasian continents, allowing for

the possibility of intercontinental immigration. Early spread to North and South America accords with a time of global aridification (Fig. 5, Peng et al., 2012; Liu et al., 2015a, 2015b). Intercontinental dispersal of the erycines might have been promoted by drying and the occurrence of a land bridge during the Miocene.

The global climate system experienced a series of drastic changes during the Cenozoic (Zachos et al., 2008). In Asia, these include the climate transformation from a zonal pattern to a monsoon-dominated pattern, the disappearance of typical subtropical flora, and the origin of inland deserts (Guo et al., 2008). The time of the earliest dispersal by members of Eryx between Africa and Eurasia was probably in the middle Miocene (~13 Ma), consistent with the development of steppe habitats in Asia and Africa driven by aridification and the expansion of the C4 grasses during the Middle and Late Miocene. (Alpers and Brimhall, 1988; Hartley and Chong, 2002; Cerling et al., 1997; Bobe, 2006; Liu et al., 2015a, 2015b; Wang et al., 2022).

4.3. Aridification in the eastern part of the Qinghai-Tibet Plateau

Many interdisciplinary studies in the eastern part of the Qinghai-Tibet Plateau have supported hypotheses of a transition to aridity since the Early Miocene, with data on color changes in the fluviolacustrine sediments, lacustrine sediments, and carbon-oxygen isotopic compositions of mammalian paleodiet (Wang and Deng, 2005; Song and Zhang, 2001; Song et al., 2007; Zhang et al., 2019; Li et al., 2020, 2021a, 2021b; Wang et al., 2022). The shift to aridity that took place in the Early Miocene might have involved various factors, such as the intensifying uplift of the Qinghai-Tibet Plateau, the strengthening of the east Asian monsoon, and the drying of the Paratethys Seaway in central Asia. (Peng, 1989; An et al., 2001, 2006; Sun and Wang, 2005; Ma et al., 1998;



Fig. 7. Reconstruction of Eryx linxiaensis in its arid habitat, Late Miocene Linxia Basin, illustrated by Qiu-Yang Zheng.

Dong et al., 2011; Liu and Dong, 2013; Sun et al., 2017; Wang et al., 2022). A recent paleomagnetic study conducted by Zhang et al. (2019) estimates the times of the environmental change in the Linxia Basin during the Miocene: forest (~21.4–16 Ma), forest-steppe (~13.8–12.5 Ma), arid steppe (~11.6–5.3 Ma), and grassland (~2.5–2.2 Ma). The age of *Eryx linxiaensis* falls in the arid steppe interval, and it likely was an arid-adapted species.

In addition to *Eryx linxiaensis*, there were several intercontinental dispersals between Africa and eastern Asia during the late Cenozoic, best represented by proboscideans (Tassy, 1986, 1990, 1994; Wang et al., 2019), rhinocerotids (Deng, 2006, 2007; van der Made, 2010; Deng et al., 2013a, 2013b, 2023), and dwarf antelopes (Wang et al., 2022).

4.4. Ecological succession in northwest China

The continued uplift of the plateau after the Late Miocene and the intensification of winter monsoons turned the warm and subarid steppe environment habitat in the Linxia Basin into a cold and seasonally humid sub-plateau environment which likely was no longer suitable for erycines (Wang et al., 1996; An et al., 2006; Dong et al., 2011; Wang et al., 2022). The continued intensification of the east Asian monsoons. together with increased dust transport to the North Pacific Ocean since the Late Pliocene (~3-2.6 Ma) led to another significant aridification event within the Asian interior (Wang et al., 1996; An, 2014; An et al., 2001, 2006, 2014; Dong et al., 2011; Liu and Dong, 2013; Tian et al., 2018; Wang et al., 2019). The vegetation type in northwestern China shifted from the sub-arid steppe to the desert (Ma et al., 1998; Tian et al., 2018), during the time estimated for the divergence among the different populations of Eryx miliaris, its occurrence may be related to this youngest aridification of the Asian interior extending from the Late Pliocene to the present.

5. Conclusions

Our study documents the first fossil record of the superfamily Booidea in China. The fossil specimen of Eryx linxiaensis sp. nov. shares many similarities with congeneric species in Africa and Asia. At the same time, it retains some plesiomorphies, such as the dorsoventrally thickened anterior part of the maxilla and the larger number of pterygoid teeth. These "primitive" characters and the phylogenetic studies both indicate the relatively early diverging position of this new erycine fossil. The results of the historical biogeographic analysis reveal that the Old World erycine clade (Eryx) probably originated in Africa and that at least three intercontinental dispersal events between Africa and Eurasia occurred. We also provide new estimates for the divergence times among the Erycidae clade suggesting Late Miocene radiation in the group.

Given the scarcity of Chinese fossil snake records, the discovery of *Eryx linxiaensis* sp. **nov.** provides the documentation of a clade previously unknown in the Chinese fossil record and it provides key information for both phylogenetic analysis and anatomy of ancient *Eryx* members. This fossil of a typically arid-adapted clade within the Yangjiashan fauna helps to reconstruct the ancient fauna and its ecological diversity (Fig. 7). Importantly, this fossil specimen of known age provides key molecular clock calibration information for future phylogenetic studies to examine the origin, evolution, and transcontinental migration of snakes (Head, 2015; Head et al., 2016). If we are to better understand intercontinental and temporal patterns of snake diversification, researchers are supposed to look to the Miocene herpetofauna of China (particularly the Linxia Basin) as a source of valuable data for phylogenetic, anatomical, and biogeographic studies.

Author contributions

Jingsong Shi, Qiang Li and Xijun Ni: Specimen collection, Writing - review & editing. Thomas A. Stidham: Writing - review & editing, language editing. Chi Zhang: Total-evidence analysis, Writing - review & editing. Qigao Jiangzuo: Ancestral geographic reconstruction. Writing - review & editing. Mo Chen, literature collection.

Jingsong Shi: conceptualization, data curation, formal analysis, funding acquisition, investigation, visualization, writing - original draft, review, editing;

Qiang Li: funding acquisition, investigation, writing - review, editing:

Thomas A. Stidham: writing - review, editing;

Chi Zhang: funding acquisition, data curation, formal analysis, methodology,

Qigao Jiangzuo: formal analysis, writing - review, editing; Mo Chen: data curation, writing - review, editing;

Xijun Ni: funding acquisition, investigation,

Declaration of Competing Interest

No conflict of interest in this study.

Data availability

No data was used for the research described in the article.

Acknowledgments

This work was funded by the Second Tibetan Plateau Scientific Expedition and Research Program (2019QZKK0705, Tao Deng and Xijun Ni), the Strategic Priority Research Program of the Chinese Academy of Sciences (XDA2007203, Tao Deng; XDB26000000, Qiang Li and Chi Zhang), the National Natural Science Foundation of China: (NSFC 42202014, Jingsong Shi; NSFC 42172029, Thomas Stidham), and the open project of State Key Laboratory of Palaeobiology and Stratigraphy: (223124, Jingsong Shi).

We are grateful to Yu Chen, Dan Lu, and Qiuyang Zheng for helping with photographing and providing the illustration, to Yemao Hou, Pengfei Yin, and Jia Wang for helping with CT scanning and 3D reconstruction, to Greg Watkins-Colwell for helping with the measurement of the specimen of *E. jaculus*, to Tao Deng, Jun Liu, Zhuding Qiu, Banyue Wang, Yan Zheng, Zhiheng Li, Boyang Sun, Xuankun Li, and Georgios L. Georgalis for their professional advice. We are grateful to Prof. Howard Falcon-Lang, Dr. Lawrence J. Flynn, and Dr. Paul Rummy for proofreading the final version of the manuscript, and to Ananjeva Natalia and David Cundall for providing important literature. We thank Dr. Jessica Maisano (UTCT) and Dr. Greg Watkins-Colwell for their kind permission to download the skull models via the website "Morphosource" (https://www.morphosource.org/).

Appendix A. Supplementary data

Supplementary data to this article can be found online at https://doi.org/10.1016/j.palaeo.2023.111491.

References

- Alpers, C., Brimhall, G., 1988. Middle Miocene climatic change in the Atacama Desert, northern Chile: Evidence from supergene mineralization at La Escondida. Geol. Soc. Am. Bull. 100, 1640–1656.
- An, Z.-S., 2014. Late Cenozoic climate change in Asia: loess, monsoon, and monsoon-arid environment evolution. Springer Science & Business Media, Dordrecht Heidelberg, New York, London, pp. 1–587.
- An, Z.-S., Kutzbach, J.E., Prell, W.L., Porter, S.C., 2001. Evolution of Asian monsoons and phased uplift of the Himalayan Tibetan plateau since Late Miocene times. Nature 411, 62–66. https://doi.org/10.1038/35075035.

- An, Z.-S., Zhang, P.-Z., Wang, E.-Q., Wang, S.-M., Qiang, X.-K., Li, L., Song, Y.-G., Chang, H., Liu, X.-D., Zhou, W.-J., Liu, W.-G., Cao, J.-J., Li, X.-Q., Shen, J., Liu, Y., Ai, L., 2006. Changes of the monsoon-arid environment in China and the growth of the Tibetan Plateau since the Miocene. Quat. Sci. 26 (5), 678-693.
- An, Z.-S., Sun, Y.-B., Chang, H., Zhang, P.-Z., Liu, X.-D., Cai, Y.-J., Jin, Z.-D., Qiao, X.-K., Zhou, W.-J., Li, L., Shi, Z.-G., Tan, L.-S., Li, X.-Q., Zhang, X.-B., Zhao, J., 2014. Late Cenozoic Climate Change in Monsoon-Arid Asia and Global Changes. Develop. Paleoenviron. Res. 16, 491–581. https://doi.org/10.1007/978-94-007-7817-7_6.
- Benson, D., Boguski, M., Lipman, D.J., Ostell, J., 1990. The National Center for Biotechnology Information. Genomics 6 (2), 389–391.
- Bien, M.N., 1934. On the fossil Pisces, Amphibia, and Reptilia from Choukoutien Localities 1 and III. Paleont Sinica, Ser C 10 (1), 14–15.
- Bobe, A., 2006. The evolution of arid ecosystems in eastern Africa. J. Arid Environ. 66, 564–584. https://doi.org/10.1016/j.jaridenv.2006.01.010.
- Bo"hme, M., 2007. Herpetofauna (Anura, Squamata) and palaeoclimatic implications: preliminary results. Wien. In: Daxner-Ho"ck, Gudrun ed. Oligocene-Miocene Vertebrates from the Valley of Lakes (Central Mongolia): Morphology, phylogenetic and stratigraphic implications – Annalen des Naturhistorisches Museum. Wien. 108 (1), 43–52.
- Burnham, K.P., Anderson, D.R., Burnham, K.P., 2002. Model Selection and Multimodel Inference: A Practical Information-Theoretic Approach. Springer-Verlag, USA.
- Cerling, E.T., Harris, J.M., Ambrose, S.H., Leakey, M.G., Solounias, N., 1997. Dietary and environmental reconstruction with stable isotope analyses of herbivore tooth enamel from the Miocene locality of Fort Ternan, Kenya. J. Hum. Evol. 33, 635–650.
- Chen, Y., Li, Y.-X., Shi, J.-S., Xie, K., 2019. Pleistocene fossil snakes (Squamata, Reptilia) from Shanyangzhai Cave, Hebei, China. Hist. Biol. 33 (5), 699–711. https://doi.org/10.1080/08912963.2019.1658094.
- Cundall, D., Irish, F., 2008. The Snake Skull. In Biology of the Reptilia. New York: Contrib. Herpetol. 23, 349–692.
- Deng, T., 2006. Paleoecological comparison between Late Miocene localities of China and Greece based on Hipparion faunas. Geodiversitas. 28 (3), 499–516.
- Deng, T., 2007. Skull of Parelasmotherium (Perissodactyla, Rhinocerotidae) from the upper Miocene in the Linxia Basin (Gansu, China). J. Vertebr. Paleontol. 27, 467– 475.
- Deng, T., Hou, S., Xie, G.-P., Wang, S.-Q., Shi, Q.-Q., Chen, S.-K., Sun, B.-Y., Lu, X., K., 2013a. Chronostratigraphic subdivision and correlation of the upper miocene of the Linxia Basin In Gansu, China. Journal of Stratigraphy. 37 (4), 417–427.
- Deng, T., Qiu, Z.-X., Wang, B.-Y., Wang, X.-M., Hou, S.-K., 2013b. In: Wang, X.-M., Flynn, L.J., Fortelius, M. (Eds.), Late Cenozoic Biostratigraphy of the Linxia Basin, Northwestern China. Columbia University Press, New York, pp. 243–273. https:// doi.org/10.7312/columbia/9780231150125.003.0009.
- Deng, T., Hou, S.-K., Wang, S.-Q., 2019. Neogene integrative stratigraphy and timescale of China. Sci. China Earth Sci. 62, 310–323. https://doi.org/10.1007/s11430-017-9155-4.
- Deng, T., Wu, F.-X., Wang, S.-Q., Su, T., Zhou, Z.-K., 2021. Major turnover of biotas across the Oligocene/Miocene boundary on the Tibetan Plateau. Palaeogeogr. Palaeoclimatol. Palaeoecol. 567, 1–12. https://doi.org/10.1016/j. palaeo.2021.110241.
- Deng, T., Lu, X.-K., Sun, D.-H., Li, S.-J., 2023. Rhinocerotoid fossils of the Linxia Basin in northwestern China as late Cenozoic biostratigraphic markers, 614, pp. 1–13. https://doi.org/10.1016/j.palaeo.2023.111427.
- Dong, M., Fang, X.-M., Ming, Q.-Z., Shi, S.-T., Su, H., 2011. Evolution of Early Pleistocene environment in Linxia Basin, Gansu Province. J. Lanzhou Univ. (Natural Sciences). 47 (1), 1–5. https://doi.org/10.13885/j.issn.0455-2059.2011.01.023. Palaeogeogr. Palaeoclimatol. Palaeoecol.
- Eskandarzadeh, N., Darvish, J., Rastegar-Pouyani, E., Ghassemzadeh, F., 2013.

 Reevaluation of the taxonomic status of sand boas of the genus *Eryx* (Daudin, 1803) (Serpentes: Boidae) in northeastern Iran. Turkish J. Zool. 37, 348–356. https://doi.org/10.3906/200-1205-1.
- Eskandarzadeh, N., Rastegar-Pouyani, N., Rastegar-Pouyani, E., Zargan, J., Hajinourmohamadi, A., Nazarov, R.A., Sami, S., Rajabizadeh, M., Nabizadeh, H., Navaian, M., 2020a. A new species of Eryx (Serpentes: Erycidae) from Iran. Zootaxa 4767, 182–192. https://doi.org/10.33256/hj30.1.212.
- Eskandarzadeh, N., Rastegar-Pouyani, N., Rastegar-Pouyani, E., Todehdehghan, F., Rajabizadeh, M., Zarrintab, M., Rhadi, F.A., Kami, H.G., 2020b. Revised classification of the genus Eryx Daudin, 1803 (Serpentes: Erycidae) in Iran and neighboring areas, based on mtDNA sequences and morphological data. Herpto. Jour. 30, 2–12. https://doi.org/10.11646/200taxa.4767.1.8.
- Georgalis, G.L., 2019. Poor but classic: The squamate fauna from the late Miocene of Pikermi, near Athens, Greece. Comptes. Rendus. Palevol. 18 (2019), 801–815.
- Georgalis, G.L., Rabi, M., Smith, K., 2021. Taxonomic revision of the snakes of the genera Palaeopython and Paleryx (Serpentes, Constrictores) from the Paleogene of Europe. Swiss J. Palaeo. 18 (2021), 1–140.
- Goloboff, P.A., Mattoni, C.I., Quinteros, A.S., 2006. Continuous characters analyzed as such. Cladistics. 22 (6), 589–601. https://doi.org/10.1111/j.1096-0031.2006.00122.x.
- Gülyüz, E., Durak, H., Oʻzkaptan, M., Krijgsman, W., 2020. Paleomagnetic constraints on the early Miocene closure of the southern Neo-Tethys (Van region; East Anatolia): Inferences for the timing of Eurasia-Arabia collision. Glob. Planet. Chang. 185 https://doi.org/10.1016/j.gloplacha.2019.103089.
- Guo, Z.-T., Sun, B., Zhang, Z.-S., Peng, S.-Z., Xiao, G.-Q., Ge, J.-Y., Hao, Q.-Z., Qiao, Y.-S., Liang, M.-Y., Liu, J.-F., Yin, Q.-Z., Wei, J.-J., 2008. A major reorganization of the Asian climate by the Early Miocene. The climate of the Past, 2008 4 (3), 153–174. https://doi.org/10.5194/cp-4-153-2008.
- Hartley, A.J., Chong, G., 2002. Late Pliocene age for the Atacama Desert: implications for the desertification of western South America. Geology 30 (1), 43–46.

- Head, J.J., 2015. Fossil calibration dates for molecular phylogenetic analysis of snakes 1: Serpentes, Alethinophidia, Boidae, Pythonidae. Palaeontologia Electronica. 18, 1–17. https://doi.org/10.26879/487.
- Head, J.J., Bloch, J.I., Hastings, A.K., Bourque, J.R., Cadena, E.A., Herrera, F.A., Polly, P. D., Jaramillo, C.A., 2009. Giant boid snake from the Palaeocene neotropics reveals hotter past equatorial temperatures. Nature (Letters). 457 (7230), 715–718. https://doi.org/10.1038/nature07671.
- Head, J.J., Mahlow, K., Müller, J., 2016. Fossil calibration dates for molecular phylogenetic analysis of snakes 2: Caenophidia, Colubroidea, Elapoidea, Colubridae. Palaeontologia Electronica. 19 (2), 1–21.
- Hecht, M.K., Hoffstetter, R., 1962. Note pr´eliminaire sur les amphibiens et les squamates du Land´enien sup´erieur et du Tongrien de Belgique. Bulletin de l'Institut royal des Sciences naturelles de Belgique. Sci. Terre 38, 1–30.
- Hoffstetter, R., Rage, J.C., 1972. Les erycinae fossiles de France (Serpentes, Boidae). Compr´ehension et histoire de la sous-famille. Ann. Pal´eont. Vert. 58, 81–124.
- Holman, J.A., 2000. Fossil Snakes of North America: Origin, Evolution, Distribution, Paleoecology. Indiana University Press, Bloomington.
- Hou, L.-H., 2005. A Miocene ostrich fossil from Gansu Province, northwest China. Chin. Sci. Bull. 50 (16), 1808.
- Hou, Y.-M., Cui, X.-D., Canul-Ku, M., Jin, S.-C., Hasimoto-Beltran, R., Guo, Q.-H., Zhu, M., 2020. ADMorph: a 3D digital microfossil morphology dataset for deep learning. IEEE Access 8, 148744–148756. https://doi.org/10.1109/ ACCESS.2020.3016267.
- Kluge, A.G., 1993. Calabaria and the phylogeny of erycine snakes. Zool. J. Linnean Soc. 107 (4), 293–351.
- LaDuke, TC., 1991. The fossil snakes of pit 91, rancho la. brea, California. Contrib. Sci. Nat. Hist. 424, 1–28. https://doi.org/10.5962/p.226807.
- Lanfear, R., Calcott, B., Ho, S.Y., Guindon, S., 2012. PartitionFinder: combined selection of partitioning schemes and substitution models for phylogenetic analyses. Mol. Biol. Evol. 29 (6), 1695–1701. https://doi.org/10.1093/molbev/mss020.
- Lanfear, R., Frandsen, P.B., Wright, A.M., Seinfeld, T., Calcott, B., 2016. PartitionFinder 2: new methods for selecting partitioned models of evolution for molecular and morphological phylogenetic analyses. Mol. Biol. Evol. https://doi.org/10.1093/ molbev/msw260.
- Li, Z.-H., Stidham, T.A., Deng, T., Zhou, Z.-H., 2020. Evidence of late miocene peritibetan aridification from the oldest asian species of sandgrouse (Aves: Pteroclidae). Front. Ecol. Evol. 8 (59), 1–10. https://doi.org/10.3389/fevo.2020.00059.
- Li, X.-K., Laurent, R.S., Earl, C., Doorenweerd, C., Nieukerken, E.J., Davis, D.R., Johns, C. A., Kawakita, A., Kobayashi, S., Zwick, A., Lopez-Vaamode, C., Ohshima, I., Kawahara, A.Y., 2021a. Phylogeny of gracillariid leaf-mining moths: evolution of larval behaviour inferred from phylogenomic and Sanger data. Cladistics. 2021, 1-24
- Li, Z.-H., Bailleul, A.M., Stidham, T.A., Wang, M., Deng, T., 2021b. Exceptional preservation of an extinct ostrich from the Late Miocene Linxia Basin of China. Vert. PalAsiatica. 59 (3), 229–244. https://doi.org/10.19615/j.cnki.1000-3118.210309.
- Li, X.-K., Hamilton, C.A., Laurent, R.S., Ballesteros-Mejia, L., Markee, A., Haxaire, J., Rougerie, R., Kitching, I.J., Kawahara, A.Y., 2022a. A diversification relay race from Caribbean-Mesoamerica to the Andes: historical biogeography of Xylophanes hawkmoths. Proc. R. Soc. B 289 (2021), 24–35. https://doi.org/10.1098/ rspb.2021.2435.
- Li, Z.-H., Stidham, T.A., Zheng, X.-T., Wang, Y., Zhao, T., Deng, T., Zhou, Z.-H., 2022b. The early evolution of diurnal habits in owls (Aves, Strigiformes) documented by a new and exquisitely preserved Miocene owl fossil from China. PNAS. 119 (15), 1–9. https://doi.org/10.1073/pnas.211921711.
- Liu, X.-D., Dong, B.-W., 2013. Influence of the Tibetan Plateau uplift on the Asian monsoon-arid environment evolution. Chin. Sci. Bull. 58 (28–29), 4277–4291. https://doi.org/10.1007/s11434-013-5987-8.
- Liu, X.-D., Sun, H., Miao, Y.-F., Dong, B.-W., Yin, Z.-Y., 2015a. Impacts of uplift of northern Tibetan Plateau and formation of Asian inland deserts on regional climate and environment. Quat. Sci. Rev. 116, 1–4. https://doi.org/10.1016/j. quascirev.2015.03.010.
- Liu, X.-D., Guo, Q.-C., Guo, Z.-T., Yin, Z.-Y., Dong, B.-W., Smith, R., 2015b. Where were the monsoon regions and arid zones in Asia prior to the Tibetan Plateau uplift? Nat. Sci. Rev. (Special Topic: The Tibetan Plateau). 2, 403–416. https://doi.org/10.1093/ ps//www.069
- Ma, Y., Li, J., Fang, X.-M., 1998. Redbed Spore-pollen Flora and climate evolution record during 30.6-5.0 Ma in Linxia Basin. Gansu. China Acad. J. 43 (3), 301–304.
- Malakhov, D.V., 2005. The Early Miocene herpetofauna of Ayakoz (Eastern Kazakhstan). Biota. 6 (1–2), 29–35.
- Matzke, N.J., 2013. BioGeoBEARS: BioGeography with Bayesian (and likelihood) evolutionary analysis in R Scripts. R package, version 0.2 1. International Biogeography Society 6th Biennial Meeting, 9-13 January 2013, Miami, Florida, USA. Abstract published in: Frontiers of Biogeography, vol. 4(suppl. 1) December 2012 (ISSN 1948-6596), p. 210. Session P10: Historical and Paleo-Biogeography. Poster 129B.
- Mccartney, J.A., Seiffert, E.R., 2015. A Late Eocene snake fauna from the Fayum Depression, Egypt. J. Vertebr. Paleont. 36 (1), 1–20. https://doi.org/10.1080/02724634.2015.1029580.
- Mead, J.L., Moscato, D., Schubert, B.W., Jin, C.-Z., Wei, G.-B., Sun, C.-K., Zheng, L.-T., 2016. Early Pleistocene snake (Squamata, Reptilia) skeleton from Renzidong Cave, Anhui, China. Hist. Biol. 28 (1-2), 208–214. https://doi.org/10.1080/08912963.2015.1023719.
- Murelaga, X., Pereda-Suberbiola, X., Rage, J.-C., Duffaud, S., Astibia, H., Badiola, A., 2002. Amphibians and reptiles from the Early Miocene of the Bardenas Reales of Navarre (Ebro Basin, Iberian Peninsula). Geobios. 35, 347–365.

- Nel, A., de Plo¨eg, G., Dejax, J., Dutheil, D., de Franceschi, D., Gheerbrant, E., Godinot, M., Hervet, S., Menier, J.J., Aug´e, M., Bignot, A., Cavagnetto, C., Duffaud, S., Gaudant, J., Hua, S., Jossang, A., Lapparent de Broin, F., de Pozzi, J.P., Paicheler, J.C., Beuchet, F., Rage, J.-C., 1999. Un gisement sparnacien exceptionnel a` plantes, arthropodes et vert´ebr´es (E´oc`ene basal, MP7): Le Quesnoy (Oise, France). Comptes Rendus de l'Acad´emie des Sciences. S´erie II Fascicule A (Sciences de la Terre et des plan`etes). 329, 65–72.
- Peng, H., 1989. A discussion on the effect of Qinghai-Tibet Plateau swelling on the climate in China. Geogr. Res. 8 (3), 85–94.
- Peng, T.-J., Li, C., Song, Z., Zhao, J., Zhang, Z. Hui, King, J.W., 2012. Biomarkers challenge Early Miocene loess and inferred Asian desertification. Geophys. Res. Lett. 39, L06702. https://doi.org/10.1029/2012GL050934.
- Pennell, M.W., Eastman, J.M., Slater, G.J., Brown, J.W., Uyeda, J.C., FitzJohn, R.G., Alfaro, M.E., Harmon, L.J., 2014. Geiger v2. 0: an expanded suite of methods for fitting macroevolutionary models to phylogenetic trees. Bioinformatics 30, 2216– 2218. https://doi.org/10.1093/bioinformatics/btu181.
- Pyron, R.A., Burbrink, F.T., Wiens, J.J., 2013. A phylogeny and revised classification of Squamata, including 4161 species of lizards and snakes. BMC Evol. Biol. 13 (1), 1–93. https://doi.org/10.1186/1471-2148-13-93.
- Pyron, R.A., Hendry, C.R., Chou, V.M., Lemmon, E.M., Lemmon, A.R., Burbrink, F.T., 2014a. Effectiveness of phylogenomic data and coalescent species-tree methods for resolving difficult nodes in the phylogeny of advanced snakes (Serpentes: Caenophidia). Mol. Phylogenet. Evol. 81, 221–231. https://doi.org/10.1016/j. ympev.2014.08.023.
- Pyron, R.A., Reynolds, R.G., Burbrink, F.T., 2014b. A taxonomic revision of boas (Serpentes: Boidae). Zootaxa. 3846 (2), 249–260. https://doi.org/10.11646/ zootaxa.3846.2.5.
- Rage, J.C., 1977. An erycine snake (Boidae) of the genus Calamagras from the French Lower Eocene, with comments on the phylogeny of the Erycinae. Herpetologica. 450–463.
- Rage, J.C., 1982. Amphibia and Squamata. Eds. Atlas, Saudi Arabia, p. 117. Revell, L.J., 2012. Phytools: an R package for phylogenetic comparative biology (and other things). Methods Ecol. Evol. 3, 217–223.
- Reynolds, R.G., Niemiller, M.L., Revell, L.J., 2014. Toward a Tree-of-Life for the boas and pythons: Multilocus species-level phylogeny with unprecedented taxon sampling. Mol. Phylogenet. Evol. 71, 201–213. https://doi.org/10.1016/j.ympev.2013.11.011.
- Rieppel, O., 1978. A functional and phylogenetic interpretation of the skull of the Erycinae (Reptilia, Serpentes). J. Zool. 186 (2), 185–208.
- Ronquist, F., Teslenko, M., van der Mark, P., Ayres, D.L., Darling, A., Ho"hna, S., Larget, B., Liu, L., Suchard, M.A., Huelsenbeck, J.P., 2012. MrBayes 3.2: efficient Bayesian phylogenetic inference and model choice across a large model space. Syst. Biol. May 61 (3), 539–542. https://doi.org/10.1093/sysbio/sys029.
- Scanferla, C.A., Smith, K.T., Schaal, S.F.K., 2016. Revision of the cranial anatomy and phylogenetic relationships of the Eocene minute boas Messelophis variatus and Messelophis ermannorum (Serpentes, Booidea). Zool. J. Linnean Soc. 176, 182–206. https://doi.org/10.1111/zoj.12300.
- Shi, J.-S., Li, J., 2023. Prehistoric snake bones from Zuojiang River Basin, Guangxi, China. Hist. Biol. 1–11 https://doi.org/10.1080/08912963.2022.2162397.
- Shi, J.-S., Wang, Y., Messger, K.R., Jiangzuo, Q.-G., Chen, Y., Jin, C.-Z., 2023. Early Pliocene fossil snakes (Squamata, Colubroidea) with various teeth from the fissure deposit in Queshan, Henan, China. Hist. Biol. 1–22. https://doi.org/10.1080/ 08912963,2022.2161382 (online).
- Smith, K.T., Scanferla, A., 2021. A nearly complete skeleton of the oldest definitive erycine boid (Messel, Germany). In: Steyer, J.-S., Aug´e, M.L., M´etais, G. (Eds.), Memorial Jean-Claude Rage: A Life of paleo-herpetologist. Geodiversitas, 43 (1), pp. 1–24. https://doi.org/10.5252/geodiversitas2021v43a1.
- Song, Y., Zhang, L., 2001. The effect of the Qinghai-Tibet Plateau uplift on the space-time distributing pattern of Chinese desert and desertification. China Populat. Res. Environ. 11 (4), 98–101.
- Song, C., Lu, X.-C., Xing, Q., Meng, Q.-Q., Xia, W.-M., Liu, P., Zhang, P., 2007. Late cenozoic element characters and palaeoclimatic change of the Lacustrine Sediments in LinxiaBasin, China. Acta Sedimentol. Sin. 25 (3), 410–416.
- Sun, A.-L., 1961. Notes on fossil snakes from Shanwang, Shantung. Vert. Paleontol. Paleoanthropol. 4, 310–312.
- Sun, X.-J., Wang, P.-X., 2005. How old is the Asian monsoon system?—Palaeobotanical records from China. Palaeogeogr. Palaeoclimatol. Palaeoecol. 222, 181–222.
- Sun, J.-M., Li, U.W.-G., Liu, Z.-H., Fu, B.-H., 2017. Effects of the Uplift of the Tibetan Plateau and Retreat of Neotethys Ocean on the Stepwise Aridification of Mid-latitude Asian Interior (Special issue: Progress of Comprehensive Scientific Research on Tibetan Plateau, China). China Acad. J. 32 (9), 951–957. https://doi.org/10.16418/jissn.1000-3045.2017.09.004.
- Sun, J.-M., Sheykh, M., Ahmadi, N., Cao, M.-M., Zhang, Z.-L., Tian, S.-C., Sha, J., Jian, Z.-M., Windley, B.-F., Talebian, M., 2021. Permanent closure of the Tethyan Seaway in the northwestern Iranian Plateau driven by cyclic sea-level fluctuations in the late Middle Miocene. Palaeogeogr. Palaeoclimatol. Palaeoecol. 564, 1–18. https://doi.org/10.1016/j.palaeo.2020.110172.
- Szyndlar, Z., 1987. Snakes from the lower Miocene locality of Dolnice (Czechoslovakia).

 J. Vert. Paleontol. 7 (1), 55–71. DOI. https://doi.org/10.1080/02724634.1987.10011637.
- Szyndlar, Z., 1991. A review of Neogene and Quaternary snakes of central and eastern Europe. Part I: Scolecophidia, Boidae, Colubrinae. Estud. Geol. 47, 103–126.
- Szyndlar, Z., 1994. Oligocene snakes of southern Germany. J. Vertebr. Paleontol. 14 (1), 24–37.
- Szyndlar, Z., Schleich, H.H., 1994. Two species of the genus *Eryx* (Serpentes; Boidae; Erycinae) from the Spanish Neogene with comments on the past distribution of the genus in Europe. Amphibia-Reptilia. 15 (3), 233–248.

- Tassy, P., 1986. Nouveaux Elephantoidea (Proboscidea, Mammalia) dans le Mioc`ene du Kenya: Essai de R´e´evaluation Syst´ematique. In: Paris: Cahiers de Pal´eontologie, E´ditions du Centre National de la Recherche Scientifique (CNRS), pp. 1–135.
- Tassy, P., 1990. The "proboscidean datum event:" how many proboscideans and how many events? In: Lindsay, E.H., Fahlbusch, V., Mein, P. (Eds.), European Neogene Mammal Chronology. Plenum Press, New York, pp. 237–252.
- Tassy, P., 1994. Gaps, parsimony, and Early Miocene elephantoids (Mammalia), with a re-evaluation of *Gomphotherium annectens* (Matsumoto, 1925). Zool. J. Linnean Soc. 112, 101–117.
- Team, R.C, 2012. R: a language and environment for statistical computing. Computing. 1, 12-21.
- Tedford, R.H., Albright, L.B., Barnosky, A.D., Ferrusquia-Villafranca, I., Hunt Jr., R.M., Storer, J.E., Swisher III, C.C., Voorhies, M.R., Webb, S.D., Whistler, D.P., 2004. Mammalian Biochronology of the Arikareean Through Hemphillian Interval (Late Oligocene Through Early Pliocene Epochs). In: Woodburne, M.O. (Ed.), Late Cretaceous and Cenozoic Mammals of North America: Biostratigraphy and Geochronology, pp. 169–231.
- Tian, Y.-Y., Wei, M.-J., Cai, M.-T., Wang, J.-P., Li, X.-L., 2018. Late Pliocene and Early Pleistocene environmental evolution from the sporopollen record of core PLo2 from the Yinchuan Basin, northwest China. Quat. Int. 476 (20), 26–33. https://doi.org/ 10.1016/j.quaint.2018.03.009.
- Tokar, A.A., 1989. 1989 A Revision of the genus $\it Eryx$ (Serpentes, Boidae). Based Upon Osteological Data Vestnik Zool. 4, 46–55.
- Tonini, J.F.R., Beard, K.H., Ferreira, R.B., Jetz, W., Pyron, R.A., 2016. Fully-sampled phylogenies of squamates reveal evolutionary patterns in threat status. Biol. Conserv. 204, 23–31. https://doi.org/10.1016/j.biocon.2016.03.039.
- Uetz, P., Hallermann, J., 2022. The Reptile Database. http://www.reptile-database.org [accessed November 2022].
- van der Made, J., 2010. The rhinos from the Middle Pleistocene of Neumark-Nord (Saxony-Anhalt). Vero "ff. Landesam. Denkmalpflege Arch" aol. 62, 433–500.
- Vasilyan, D., Zazhigin, V.S., Bohme, M., 2017. Neogene amphibians and reptiles (Caudata, Anura, Gekkota, Lacertilia, and Testudines) from the south of Western Siberia, Russia, and Northeastern Kazakhstan. PeerJ. 5 (e3025), 1–65. https://doi. org/10.7717/peerj.3025.
- Volume Graphics GmbH, 2017. Volume graphics releases structural mechanics simulation for VGStudio MAX 3.0. e-J. Nondestruct. Test. 22 (1). https://www.ndt. net/?id=20632.
- Wang, Y., Deng, T., 2005. A 25 m.y. isotopic record of paleodiet and environmental change from fossil mammals and paleosols from the NE margin of the Tibetan Plateau. Earth Planet. Sci. Lett. 236 (1-2), 322–338.
- Wang, B.-Y., Qiu, Z.-X., 2018. Late Miocene Pararhizomines from Linxia Basin of Gansu, China. Science Press, Beijing, 1—.
- Wang, X.-T., Song, Z.-M., Yang, Y.-T., Liu, N.-F., Chen, J.-C., Zhang, S.-Z., Wang, D.-Q., 1981. Study on the avifauna of Gansu Province, China. J. Lanzhou Univ. (Natural Sciences). 3 (14), 114–125.

- Wang, Y., Li, S., Wang, J.-H., Yan, M.-C., 1996. The uplift of the Qinghai-Xizang (Tibetan) Plateau and its effect on the formation and Evolution of Chinese Deserts. Arid Zone Res. 13 (2), 21–24. https://doi.org/10.13866/j.arz.1996.02.002.
- Wang, S.-Q., Li, C.-X., Zhang, X.-X., Jiangzuo, Q.-G., Ye, J., Li, L., Li, F.-C., 2019. A record of the early *Protanancus* and *Stephanocemas* from the north of the Junggar Basin, and its implication for the Chinese Shanwangian. Vertebrata PalAsiatica 57 (2),
- Wang, S.-Q., Sun, J.-M., Li, C.-X., Li, S.-J., Fu, J., Jiangzuo, Q.-G., Xing, L.-D., Yang, R., 2022. Discovery of a fossil dwarf antelope outside of Africa and its implications for the Late Miocene ecosystem in the northeast margin of the Tibetan PlateauGondwana Research, 113 (2023), 102–115. https://doi.org/10.1016/j.gr.2022.10.012.
- Yao, C.-Y., 2004. Reptilian fauna and zoogeographic division of Gansu Province. Sichuan J. Zool. 23 (3), 217–221.
- Yu, Y., Blair, C., He, X., 2020. RASP 4: Ancestral State Reconstruction Tool for Multiple Genes and Characters. Mol. Biol. Evol. 37 (2), 604–606. https://doi.org/10.1093/ molbev/msz257.
- Yu, Y., Harris, A.J., Blair, C., He, X., 2015. RASP (Reconstruct Ancestral State in Phylogenies): a tool for historical biogeography. Mol. Phylogenet. Evol. 87, 46–49. https://doi.org/10.1016/j.ympev.2015.03.008.
- Zachos, J.C., Gerald, R.D., Richard, E.Z., 2008. An early Cenozoic perspective on greenhouse: warming and carbon-cycle dynamics. Nature 451 (17), 279–283.
- Zaher, H., Murphy, R.W., Arredondo, J.C., Graboski, R., Machado-Filho, P.R., Mahlow, K., Montingeli, G., Quadros, A.B., Orlov, N.L., Wilkinson, M., Zhang, Y.P., Grazziotin, F., 2019. Large-scale molecular phylogeny, morphology, divergence-time estimation, and the fossil record of advanced caenophidian snakes (Squamata: Serpentes). PLoS One 14 (5), e0216148. https://doi.org/10.1371/journal.
- Zhang, C., 2019. Molecular clock dating using MrBayes. Vert.Pala. 57 (3), 241–252. https://doi.org/10.19615/j.cnki.1000-3118.190408.
- Zhang, C., 2021. Using Bayesian tip-dating method to estimate divergence times and evolutionary rates. Vert.Pala. 59 (4), 333–341.
- Zhang, Z., Zheng, X., Zheng, G., Hou, L.-H., 2009. A new Old World vulture (Falconiformes: Accipitridae) from the Miocene of Gansu Province, northwest China. J. Ornithol. 151 (2), 401–408. https://doi.org/10.1007/s10336-009-0468-1.
- Zhang, W.-L., Erwin, A., Wang, J.-Y., Fang, X.-M., Zan, J.-B., Yang, Y.-B., Miao, Y.-F., Yan, X.-L., 2019. New paleomagnetic constraints for *Platybelodon* and Hipparion faunas in the Linxia Basin and their ecological environmental implications. Glob. Planet. Chang. 176, 71–83. https://doi.org/10.1016/j.gloplacha.2019.03.002.
- Zhao, E.-M., 2006. Snakes of China. Anhui Science and Technology Publishing House, Anhui: Hefei, pp. 112–114.
- Zhao, E.-M., Zhong, Y., Huang, M.-H., 1998. Fauna Sinica. Reptilia. Science Press, Beijing, China, pp. 33–34.